Nature Environment and Pollution Technology
An International Quarterly Scientific Journal

p-ISSN: 0972-6268
(Print copies up to 2016)
e-ISSN: 2395-3454

Vol. 24 | No. 4 | Article ID D1774 | 2025

Original Research Paper

https://doi.org/10.46488/NEPT.2025.v24i04.D1774

Open Access Journal

Modelling the Future: Groundwater Responses to Climate Change in Talomo-Lipadas Watershed, Davao City, Philippines

Nympha Ellarina-Branzuela†
Department of Forestry, CARS, University of Southeastern Philippines (USeP),Tagum-Mabini Campus, Municipality of Mabini, Davao de Oro, Philippines
†Corresponding author: Nympha Ellarina-Branzuela; nympha.branzuela@usep.edu.ph

Abbreviation: Nat. Env. & Poll. Technol.
Website: www.neptjournal.com

Received: 09-02-2025
Revised: 10-04-2025
Accepted: 14-04-2025

Key Words:

Climate change
Statistical downscaling method
BROOK90 hydrological model
Groundwater recharge
Talomo-Lipadas Watersheds

Citation for the Paper:

Ellarina-Branzuela, N., 2025. Modelling the future: Groundwater responses to climate change in Talomo-Lipadas watershed, Davao City, Philippines. *Nature Environment and Pollution Technology*, 24(4), D1774. https://doi.org/10.46488/NEPT.2025.v24i04.D1774

Note: From 2025, the journal has adopted the use of Article IDs in citations instead of traditional consecutive page numbers. Each article is now given individual page ranges starting from page 1.

ABSTRACT

This research investigates the long-term impact of climate change on groundwater recharge (seepage) within the Talomo-Lipadas Watershed, Davao City, Philippines, over the next eighty-nine (89) years. Employing the Statistical Downscaling Method (SDSM), station-scale climate scenarios were generated for three future time slices centered on 2020 (2011-20140), 2050 (2041-2070), and 2080 (2071-2100). These scenarios, indicating a projected increase in temperature within the watershed, were then used as input for the BROOK90 hydrological model to simulate groundwater recharge. The modelling results project a decline in groundwater supply from 109.01 million cubic meters (MCM) in 2020 to 103.53 MCM in 2050 and further down to 99.81 MCM by 2080. This projected decrease in groundwater recharge has significant implications beyond just water availability. Reduced groundwater flow can impact baseflow in rivers, affecting aquatic ecosystems and potentially exacerbating water scarcity during dry periods. Decreased recharge also has implications for other water-related sectors, including agriculture (irrigation), industry (water supply), and domestic water use, potentially leading to increased competition for dwindling resources. These findings underscore the urgent need for adaptation strategies to mitigate the effects of climate change on groundwater recharge within the Talomo-Lipadas Watershed. Further research employing diverse hydrological models is recommended to validate these findings and provide a more robust basis for developing sustainable water management plans.

INTRODUCTION

Climate change significantly disrupts watershed hydrodynamics globally, destabilizing vital water systems underpinning agriculture, ecosystem stability, and human survival. Groundwater storage, a cornerstone of freshwater sustainability (Wu et al. 2020), faces mounting threats to its availability and quality (Dao et al. 2024) due to its inherent sensitivity to the changing climate, with the manifestation of these effects intensifying in recent years (Bamala et al. 2024).

The quantifiable trends in global climate parameters demonstrate the persistence of climate change, with its consequent impacts now evident in localized environmental responses. Observational data and climate projections provide abundant evidence that freshwater resources (both surface and groundwater resources) are vulnerable and have the potential to be strongly affected by climate change, with wide-ranging consequences for society and ecosystems (Bates et al. 2008). Understanding climate-change effects on groundwater is unknown and has not been explored sufficiently, because climate change may affect hydrogeological processes and groundwater resources directly and indirectly (Dettinger & Earman 2007).

Despite growing climate change impact research, substantial knowledge gaps persist, particularly regarding localized watershed effects and the understudied groundwater resources in vulnerable regions like the Philippines. Advanced hydrological modelling is crucial for accurately assessing climate-driven

groundwater storage changes, highlighting the necessity for sophisticated, region-specific research.

While recent studies (Ficklin et al. 2018, Davamani et al. 2024, Benz et al. 2024) have established climate change's disruptive influence on watersheds, demonstrating altered hydrology, ecosystem degradation, and strain on human systems, significant knowledge gaps persist. Specifically, the precise mechanisms by which climate change modifies groundwater recharge, discharge, and temperature, and the subsequent cascading effects on hydrological processes and water quality, require further investigation. For instance, while Benz et al. (2024) project a 2.1% groundwater temperature increase under a medium emissions scenario, the regional variability and long-term consequences of this warming on specific aquifer systems remain underexplored.

More scientists used models in studies of predicting hydrologic implications on climate change impacts (Flatto & Boer 2001, Combalicer et al. 2011, Nyeko-Ogiramo, 2010, Zachary Pirtle et al. 2010). Of particular interest among climate change researchers and groundwater specialists is the use of the Statistical Downscaling Method (SDSM) in determining the station-scale climate scenario and BROOK90 hydrological modelling (Federer et al. 2003) in determining the groundwater (recharge) availability of a particular watershed area. The SDSM model can produce localized, station-scale climate data from broader GCM output and generate daily weather sequences, although it does not incorporate leap years in its calculations (Combalicer et al. 2010).

BROOK90 excels in localized studies requiring detailed analysis of soil water dynamics and evapotranspiration (Federer et al. 2003), as demonstrated by Vorobevskii (2020) in estimating vertical water fluxes within small-scale (under 100 km²) soil-water-plant systems, while also offering an automated framework for broader water balance simulations. This detailed representation contrasts with other hydrological models like SWAT (Kiniry 2012), which employ simplified groundwater representations and have limitations in simulating lateral flow.

For this study, the A2 scenario or 'business as usual' was chosen to represent a high-end, but plausible, future emissions trajectory. It assumed a heterogeneous world with regionally oriented economic development, a continuously growing global population, and slower technological change. It was used to explore the potential consequences of a future where emissions were not significantly mitigated. Considering the site-specific area of the Philippines, which is more likely to be compared to this scenario rather than the RCP scenario.

Davao City, Philippines, consists of eight subwatersheds. The Davao River Basin has an estimated drainage area of more or less 1,700 square kilometers, with an estimated length of 138 kilometers. Out of eight subwatersheds, the Talomo- Lipadas Watersheds have been prioritized for management, where they supply 99 of % urban population of drinking water (Hearne 2011). By 2025, Davao City's water supply is projected to be 45% below demand compared to 1995 levels, according to the Philippines Environment Monitor (2003). This significant deficit is linked to a decrease in projected groundwater availability to 84 million cubic meters per year from 153 million cubic meters per year in 1995. The National Water Regulatory Board (NWRB) has also identified Davao City as a water-critical area.

Despite growing attention to the broad impacts of climate change, our understanding of its specific, localized effects on watersheds and groundwater resources remains critically limited, particularly within vulnerable nations such as the Philippines, and even more so in specific regions like Davao City. Accurately assessing climate-driven changes in groundwater storage necessitates the application of advanced hydrological modelling and underscores the urgent need for in-depth, region-specific research to address this significant knowledge deficit.

MATERIALS AND METHODS

The study employed two open-source software, namely, the Statistical Downscaling Method (SDSM) and BROOK90 hydrological modelling. SDSM simulates the eighty-nine (89) years station-scale climate projections using the work of Branzuela et al. (2015).

Groundwater availability was simulated using the BROOK90 hydrological model. This study prioritizes the Talomo and Lipadas sub-watershed (shown in Fig. 1) due to their vital role in supplying water to Davao City. These sub-watersheds are the primary recharge areas for the city's groundwater, with Lipadas being the core site for the Davao City Water District's production wells. Their combined 38,374-hectare area spans the Baguio, Calinan, Toril, Talomo, and Tugbok districts.

Statistical Downscaling Method

Local information was sourced from the Agrometeorological Station for the predictand, while larger-scale data sets from the National Centre for Environmental Prediction (NCEP) served as predictors- these models were subsequently utilized with GCM-derived predictors to generate daily weather data for a future timeframe (Wilby et al. 2002).

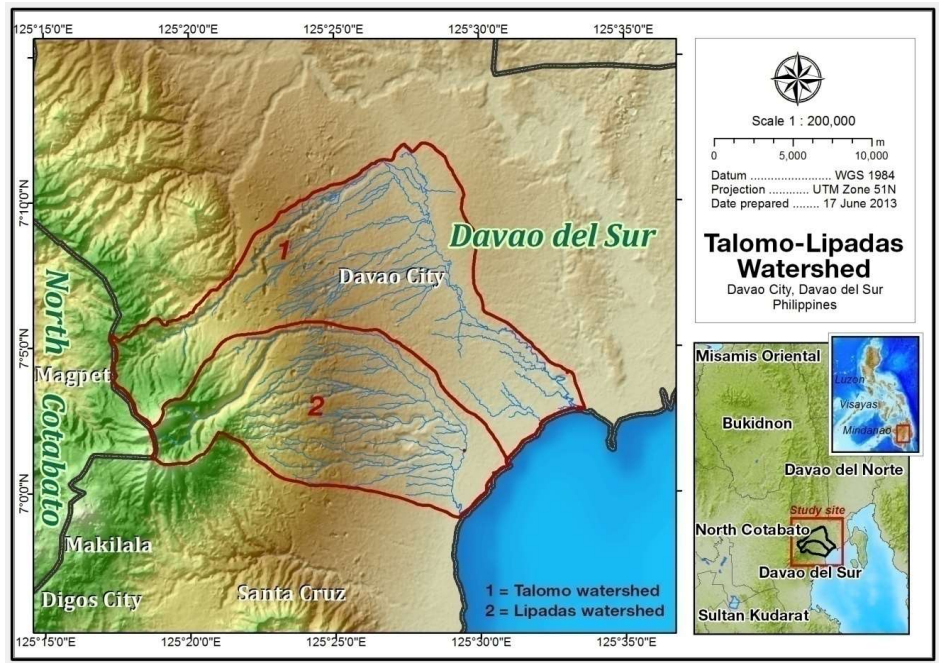

Fig. 1: Location of the Study.

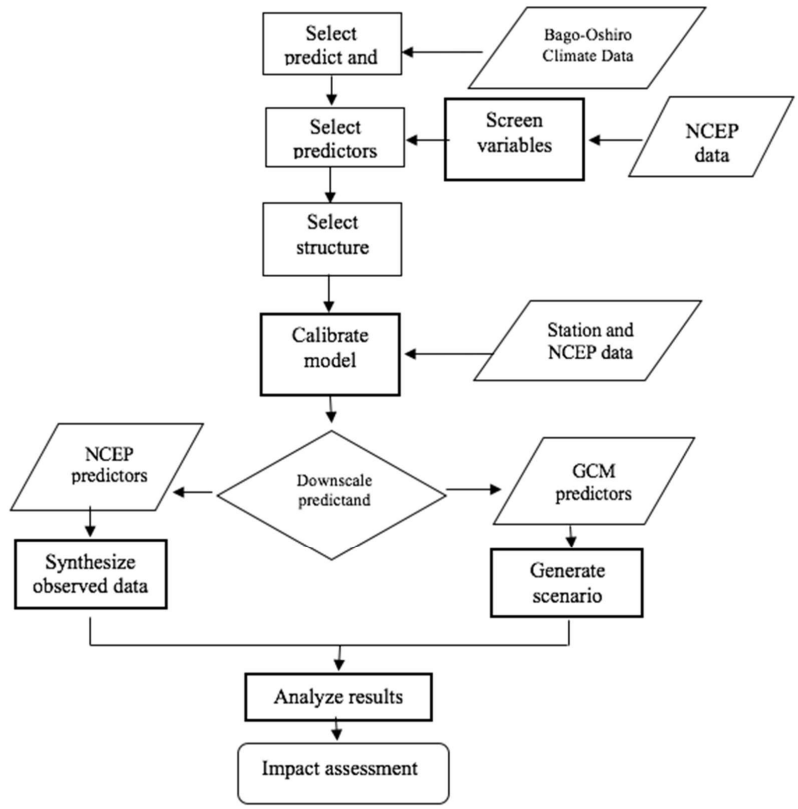

Source: Wilby et al. (2002)

Fig. 2: SDSM Climate Scenario Generation Process.

The SDSM serves as a decision support instrument for evaluating the effects of climate change at the local level by utilizing a robust statistical downscaling method. SDSM enables users to identify significant large-scale climate variables (the predictors) that account for the majority of variability in the climate (the predictand) at a particular site, specifically within the two sub-watersheds, and statistical models are subsequently developed based on this data. Again, this process can be accessed in the previous publication of Branzuela et al. (2015). Fig. 2 describes the generation processes.

Predictor variables were carefully selected based on a correlation analysis with the predictand variables over 12 months, using a 95% confidence level. The chosen predictors were also evaluated for their conceptual and physical relevance to the local weather site. Table 1 demonstrates a strong correlation between these predictors and the predictands at the local weather station in Bago Oshiro. For minimum temperature (Tmin), eight out of twenty-six potential predictors showed high correlation, including p, z, p_th, p5_f, 850 hPa, p8th, s500, s850, and temp. For maximum temperature (Tmax), eight out of twenty-six identified predictors were highly sensitive in downscaling, namely: slpg, p, p_th, p500, p5th, p5zh, s850, shum, and temp. For precipitation, seven out of twenty-six predictors exhibited high correlation with the predictand, specifically: slpg, p, u, p5, p500, p5zh, p8th, and p8zh.

Table 1: List of predictors from NCEP and CGCM3 datasets and selected predictors that correlate highly with each predictor.

Predictors Code	Description	Predictands		
		TMIN	TMAX	RAIN
Slpg	Mean sea level pressure		X	X
p f	1000 hPa Wind speed			
p u	1000 hPa U-component			X
p v	1000 hPa V-component			
p z	1000 hPa Vorticity	X		
p_th	1000 hPa Wind direction	X	X	
p_zh	1000 hPa Divergence			
p5_f	500 hPa Wind speed	X		
p5_u	500 hPa U-component			X
p5_v	500 hPa V-component			
p5_z	500 hPa Vorticity			
p500	500 hPa Geopotential		X	X
p5th	500 hPa Wind direction		X	
p5zh	500 hPa Divergence		X	X
p8_f	850 hPa Wind speed			
p8_u	850 hPa U-component			
p8_v	850 hPa V-component			
p8_z	850 hPa Vorticity			
p850	850 hPa Geopotential	X		
p8th	850 hPa Wind direction	X		X
p8zh	850 hPa Divergence			X
s500	500 hPa Specific humidity	X		
s850	850 Specific humidity	X	X	
Shum	1000 hPa Specific humidity		X	
Temp	Temperature at 2m	X	X	
Prcp	Accumulated precipitation			

Groundwater Modelling Using BROOK90 Hydrological Model

First, hydrologic secondary data, the gage height and water discharge gathered at the office of Materials Quality Control and Hydrology Division, Department of Public Works and Highways (DPWH), Davao City. The office takes charge of monitoring the streamflow of the said watersheds, which measures the gage height of the water level three times a day. Streamflow data were monitored from 1980 up to the present.

Second, the next underlying process is the land cover analysis, in which both the normalized difference vegetation index (NDVI I4.7) and the ArcGIS software were used to process reclassified land cover. These two processes are vital in determining the water budget.

The water budget is generated using the BROOK90 hydrologic model. Water budget is used to simulate daily evaporation and soil-water movement using a process-oriented approach for a single forest stand/site or a small watershed, with some provision for runoff (streamflow) generation by different flow paths (Federer et al. 2003). To account for varying land cover across the two watersheds, four simulation runs were conducted, each using parameter values tailored to a specific land cover classification. The generated simulated flow is the average of four land cover types. Precipitation is a function of streamflow, evaporation loss, and deep seepage. Datasets were divided into the calibration period and the validation period. Results were subjected to sensitivity analysis to determine the changes in the value of parameters and changes in structure (Combalicer et al. 2010).

BROOK90 is particularly beneficial for detailed investigations of soil water dynamics and evapotranspiration at a localized scale, as demonstrated by Vorobevskii (2020), who utilized it with new R functionalities to estimate vertical water fluxes within the soil-water-plant system of a single site or a small catchment (under 100 km²). Furthermore, BROOK90 offers an automated framework for simulating

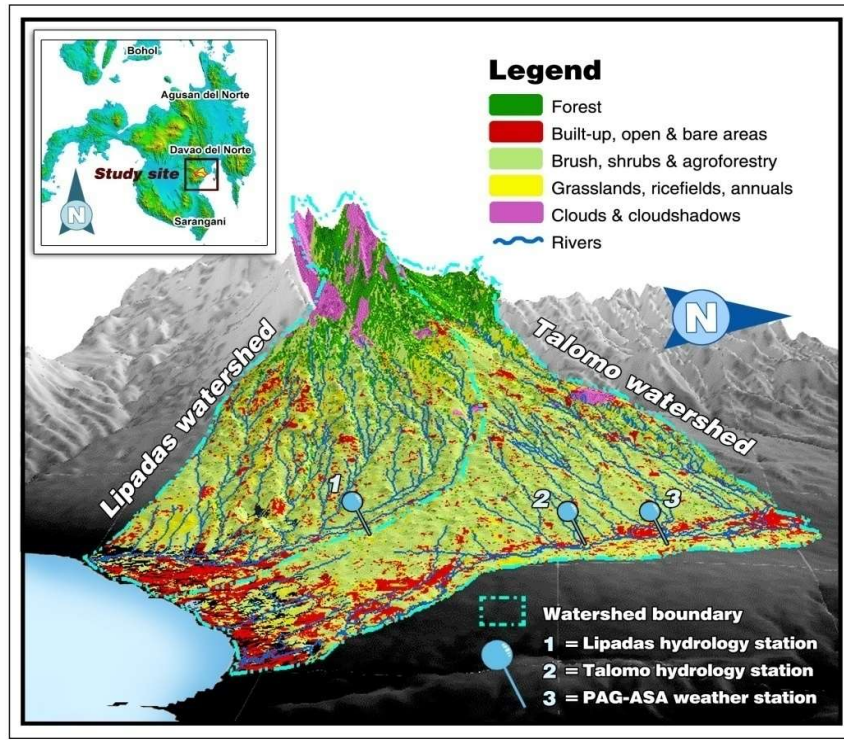

Fig. 3: Land cover map of Talomo-Lipadas, PAGASA weather station and hydrology station.

water balance at any given location. However, there are other hydrological software alternatives like SWAT (Kiniry 2012) that represent simplified groundwater representations and lateral flow limitations.

Fig. 3 shows the meteorological and hydrological stations within the study area. Meteorological inputs are the simulated climate data (daily precipitation, temperature maximum, temperature minimum, and sunshine duration) generated from SDSM. The PAGASA weather station is located at 07°04' 06" latitude and 125°27'99" longitude (Fig. 3). Ten (10) years of streamflow data were taken in both the Talomo River and the Lipadas River as monitored and archived by the DPWH in Davao City. The regional office of the Department of Environment and Natural Resources Office (DENR XI), also located in Davao City, was the source of the maps and shapefiles employed in this research.

The BROOK90 hydrological model requires six parameters: flow, location, drainage, canopy, soil, and initial conditions. These parameters were carefully adjusted to calibrate the model for accurate discharge simulation in the two watersheds. A sensitivity analysis, particularly RMSE and Nash-Sutcliffe, was performed on the measured and simulated discharges to evaluate model fit. Additionally, monthly and yearly water balance analyses were conducted. Fig. 4 illustrates these essential BROOK90 parameters.

Location parameters: This section describes site-specific parameters used in the study, focusing on location and environmental factors. For the Talomo site, the latitude is 7.08, while for Lipadas it is 7.09. The degree slope for evapotranspiration is 34.45 in Talomo and 34.23 in Lipadas. A snow-rain transition temperature of -0.5 and a degree-day melt factor for open land of 1.5 were used. Relative height and relative leaf area index (an array of ten-day-of-year and relative LAI values between 0 and 1) are also specified. Finally, (DURATN), representing the average duration of daily precipitation per month, is included as a parameter.

Flow parameters: In this model, water infiltration is controlled by two parameters: INFEXP and IDEPTH. Setting both to zero simulates a basic top-down infiltration process. Specifically, IDEPTH controls the number of soil layers that receive infiltrated water, while INFEXP determines the distribution of that water within the soil layers. Table 1 represents the final values used for the flow meter.

Canopy parameters: Several parameters related to the forest canopy and land surface are critical for determining how quickly trees transpire, as reflected in Table 2. These include the surface albedo (reflectivity) under both snow-free (ALB) and snow-covered (ALBSN) conditions, which may be known for specific locations. The relative density of tree roots (ROOTDEN) is another important factor. Additionally,

Table 1: Final Values for Flow Parameter.

Parameters	Description	Range	Final Values
IDEPTH	Depth over which infiltration is distributed	> 0	1,000
INFEXP	Infiltration exponent that determines the distribution of infiltrated water with depth, (f)	0 - 1.0	1.0
IMPERV	The fraction of the soil surface that is impermeable and always routes water reaching it directly to streamflow	0 - 1	0.01
BYPAR	Bypass flow from deeper layers	0 - 1	0
QDEPTH	Soil depth for SRFL calculation (mm)	≥ 0	1,000
QFPAR	Fraction of the water content between field capacity (THETAF) and saturation (THSAT) at which the quick flow fraction is 1, (f)	0.2 - 5	1
QFFC	Quick flow fraction for SRFL and BYFL at THETAF, (f)	0.02 – 0.3	0.05
LENGTH	Slope length for downslope flow (m)	≥ 0	10000
DSLOPE	Downslope, (deg)	≥ 0	4
DRAIN	Multiplier between 0 and 1 of drainage from the lowest soil layer, (f)	0 - 1	0.01
GSC	Fraction of groundwater storage (GWAT), that is transferred to groundwater (GWFL) and deep, seepage (SEEP) each day, (f)	0.005 – 0.5	0.003
GSP	Fraction of groundwater (discharge, (f)	≥ 0	0

the fraction of plant resistance located within the xylem tissue (FXYLEM) plays a role, as this parameter, in conjunction with ROOTDEN, controls the amount of transpiration occurring in each soil layer. Finally, the maximum height of the forest canopy (MAXHT) and the maximum projected leaf area index (MAXLAI) are considered. MAXLAI is influenced by the density of the forest at a given site.

In modelling climate change impacts on hydrological processes, the canopy parameter variables were run four (4) times per land cover type (Table 3). Each canopy parameter was adjusted (Federer 2014) to obtain reasonable values per land cover type. The four land cover types represent the simulated flow of the area.

Soil parameters: This section describes soil profile and water property parameters used in the BROOK90 model, emphasizing the influence of the number of soil layers as shown in Table 4. NLAYER defines the number of soil layers, while THICK specifies the thickness of each layer. Key parameters include: hydraulic conductivity at field capacity (KF, in mm/d), volumetric water content at field capacity (THETAF), and matric potential at field capacity (PSIF). RELDEN represents the relative root density per unit volume (m3/m3), STONEF is the stone volume fraction,

Table 2: Final Values for Canopy Parameter.

Parameters	Description	Range of Values	Final Values
ALB	Albedo	0.1 – 0.3	0.23
ALBSN	Surface reflectivity without and with snow on the ground [f]	0.1 – 0.9	0.35
KSNVP	Multiplier to reduce snow evaporation, arbitrary [f]	0.2 – 2.0	0.3
Z0G	Ground surface roughness [m]	≥ 0.001	0.02
MAXHT	Maximum canopy height for the year [m]	▯ 0.01	50
MAXLAI	Maximum projected LAI for the year [m^2m^{-2}]	▯ 0.00001	6
MXRTLN	Maximum length of fine roots per unit ground area $m.m^{-2}$]	1700 – 11000	3500
MXKPL	Maximum plant conductivity [mmd^{-1} Mpa^{-1})	5-30	8
FXYLEM	Fraction of the internal plant resistance to water flow that is in the xylem [f]	0 – 0.99	0.5
CS	Ratio of projected stem area index (SAI) to HEIGHT [f]	≥ 0	0/35
PSICR	Minimum plant leaf [Mpa]	-15 – 20	-2
GLMAX	Maximum leaf conductance [$cm.s^-$]	0.2 – 2.0	0.57
LWIDTH	Average leaf width [m]	▯ 0.01	0.08
CR	Extinction coefficient for photosynthesis-active radiation in the canopy [f]	0.5 – 0.7	0.6

Source: Combalicer et al. (2010)

Table 3: Final Values for Each Land Cover Type.

Parameters	Forest	Brush	Grassland	Bare
ALB	0.25	0.62	0.09	0.16
ALBSN	0.23	0.5	0.45	0.35
KSNVP	0.3	1	.3	.3
Z0G	0.02	0.02	0.02	0.02
MAXHT	30	.3	10	10
MAXLAI	6	3	6	6
MXRTLN	3500	110	2000	100
MXKPL	15	8	8	8
FXYLEM	0.5	0	0.5	0.5
CS	0.035	0.035	0.035	0.035
PSICR	-2	-2	-2	-2
GLMAX	0.53	1.1	0.5	0.5
LWIDTH	0.1	0.1	0.05	0.05
CR	0.6	0.7	0.6	0.6

and WETINF denotes the wetness at the dry end of the near-saturation range. Finally, PSIM specifies the initial matric soil water potential (kPa) for each layer.

Fixed parameters: These are constant values established based on a range of sources, and there are no recommendations provided for altering them.

Initial parameters: All the parameters can be configured to a value of 0, except PSIM, which may be -10 kPa. Typically, an initializing period, often spanning a year, is executed to mitigate the impact of initial values. In BROOK90, this process is facilitated through the 'number of initialization days' feature on the main screen. Each parameter's values were properly adjusted to accurately measure and calibrate the discharges in the two watersheds. Results of measured and simulated water discharges were subjected to sensitivity analysis to determine the model's fitness. Water balance analysis was then simulated monthly and yearly.

Table 4: Final Values for Soil Parameter.

Layer No	Soil Depth (THICK), mm	Stone volume fraction [STONE], f	Matrix potential [PSIF], kPa	Volumetric water content [THETAF], $m^3.m^{-3}$	Matrix porosity [THSAT], $m^3.m^{-3}$	Negative slope of the log psi [BEXP]	Hydraulic conductivity (KF), mm.d^{-}
1	200	0	-6.0	0.397	0.60	7.75	4.9
2	400	0	-7.7	0.425	0.60	11.4	4.3
3	600	0	-7.7	0.425	0.60	11.4	4.3
4	800	0	-7.7	0.425	0.60	11.4	4.3
5	1000	0	-6.5	0.433	0.60	10.4	4.2

Source: Combalicer 2010

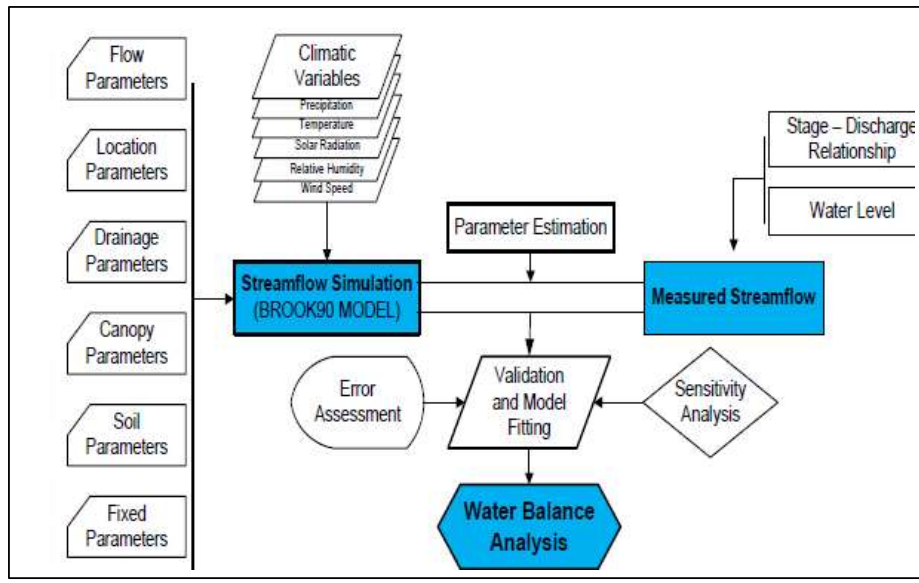

Source: Combalicer, 2010

Fig. 4: Parameters used in the BROOK90 Model.

RESULTS AND DISCUSSION

Local Climate Projection using Statistical Downscaling Method (SDSM)

Statistical Downscaling Model (SDSM) was employed to generate present and future climate scenarios centered on the three time slice periods at 2020 (2011-2040), 2050 (2041-2070) and 2080 (2071-2100). Calibration and validation processes were carried out to identify the most fitting model for projecting climate scenarios. Model calibration involved the creation of monthly structured models, utilizing twelve distinct regression models, each representing a specific month and incorporating various parameters.

The calibration process spanned a period of 20 years (1976-1995), while model validation encompassed 12 years (1989-2000), as shown in Table 5. The data sets were divided based on the methodologies outlined by Kozak & Kozak (2003), which advocate for the implementation of cross-validation and double cross-validation to enhance the reliability of information derived from the data. In both calibration and validation figures, the line graph demonstrates a strong agreement between the observed and simulated data of minimum and maximum temperature and precipitation.

Improved concordance was achieved due to the minimal disparity between the observed data and residual or simulated data. The calculated RMSE and MAE were lower in minimum (Tmin) and maximum temperature (Tmax) compared to the rainfall during the calibration and validation processes.

Table 6 presents the projected minimum temperatures (Tmin) under future climate scenarios of 2020, 2050, and 2080 and their increase/decrease relative to observed values (Fig. 5). The Tmin fluctuates slightly but generally shows an increasing trend over time. Some months, like March, April, and November, show slight cooling in later projections (2080), while others, May and July, exhibit warming temperatures. Higher minimum temperatures are observed in March, April, May, June, September and October. While July and August have the lowest Tmin. Global climate models under the A2 scenario, minimum temperatures will increase (IPCC 2021). Higher minimum temperatures can disrupt plant growth cycles, particularly in tropical and subtropical regions (Hatfield & Prueger 2015). Warming nights reduce cooling periods for crops, impacting yield quality and production (Rosenzweig et al. 2001). Countries dependent on rain-fed agriculture may face drought risks due to increased evaporation (Christensen et al. 2007).

Table 5: Summarize model evaluation criteria.

	Rainfall		TMIN		TMAX	
	Calibration	Validation	Calibration	Validation	Calibration	Validation
RMSE	13.12	14.81	1.57	1.62	1.32	1.49
MAE	7.57	8.32	1.17	1.16	0.96	1.07
E	-0.0173	0.0237	0.0853	0.1220	0.0902	0.1212

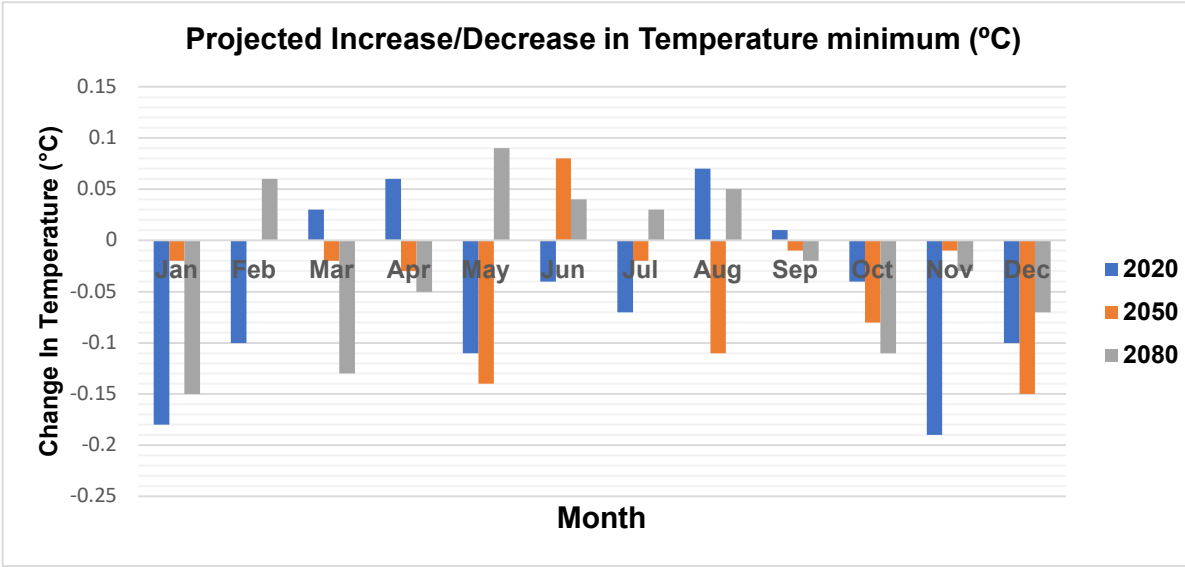

Fig. 5: Projected changes in mean monthly minimum temperature (°C).

Table 6: Mean monthly comparison and rate of change (increase/decrease) on the minimum temperature.

Month	Observed data	Temperature Minimum					
		Centigrade [^{o}C]			Increase/Decrease		
		2020	2050	2080	2020	2050	2080
Jan	21.39	21.20	21.37	21.24	**-0.18**	**-0.02**	**-0.15**
Feb	21.78	21.68	21.78	21.84	**-0.10**	0.00	0.06
Mar	22.14	22.17	22.12	22.01	0.03	**-0.02**	**-0.13**
Apr	21.93	21.99	21.90	21.88	0.06	**-0.03**	**-0.05**
May	22.05	21.94	21.91	22.15	**-0.11**	**-0.14**	0.09
Jun	21.38	21.34	21.46	21.42	**-0.04**	0.08	0.04
Jul	20.89	20.81	20.86	20.91	**-0.07**	**-0.02**	0.03
Aug	21.07	21.14	20.96	21.11	0.07	**-0.11**	0.05
Sep	21.09	21.10	21.08	21.07	0.01	**-0.01**	**-0.02**
Oct	21.07	21.03	20.98	20.96	**-0.04**	**-0.08**	**-0.11**
Nov	21.39	21.20	21.38	21.36	**-0.19**	**-0.01**	**-0.03**
Dec	21.21	21.10	21.06	21.14	**-0.10**	-0.15	-0.07

Fig. 5 shows the graphical representation of the trends over time.

Fig. 6 depicts the projected mean monthly maximum temperature (Tmax) for Talomo-Lipadas Watersheds. There is a most striking feature of the projected temperatures for both 2020 and 2050's which have generally higher Tmax from the observed temperatures across all months. Table 7 depicts in numerical values of the increase and decrease of Tmax, which clearly indicates a future warming trend in the said watersheds. The degree of warming appears to intensify from the 2020s to the 2050s, suggesting a progressive increase in Tmax over time as climate impacts become more pronounced. While the overall trends in warming, the figure, as well as the numerical increase/decrease, as shown in Table 7, the increases vary across different months. It is crucial to examine the seasonal changes to understand their potential impacts on specific ecological processes and human activities. For instance, the months of March to May exhibit the highest projected temperatures, which could exacerbate drought conditions. Increased Tmax can lead to higher evapotranspiration rates, potentially reducing soil moisture and impacting water availability for both natural ecosystems and human use. Parmesan and Yohe (2023) stated that rising temperatures can disrupt ecological processes, affecting species distribution, phenology, and ecosystem productivity. Warmer temperatures can also favour invasive species and increase the risk of pest and disease outbreaks. Agriculture is highly sensitive to temperature changes. Increased maximum temperatures can reduce crop yields, particularly for heat-sensitive crops. Change in temperature patterns can also affect the timing of planting and harvesting, potentially disrupting agricultural practices (Tubiello 2007).

Subsequently, this potential temperature increase would bring immense changes to the hydrological processes and vegetation responses. Plants are highly dependent on climatic conditions; hence, the "sponge" effect of the forest will be affected with the potential increase in temperature. This will imply for the climate-dependent sectors, especially among domestic water users, agricultural water users, commercial and industrial users, among others.

As to precipitation, the three slice time periods 2020, 2050 and 2050 show consistently more and heavier rain with a remarkable increase in January. All three time slice periods show a significant increase of 38.79%, 28.15% and 24.84%, respectively, compared to the observed data.

The results of this study, based on statistical downscaling, contradicted PAGASA's (2011, p. 42) future rainfall projections obtained via dynamical downscaling. According to PAGASA's medium-range emission scenario, rainfall was not expected to surpass 300 mm in 2020 and 2050, a finding that differs from the current analysis. The statistical downscaling method has projected an increase of over 300mm (about 11.81 in) specifically for June (335 mm), especially in the 2050 sliced period. This validation process will identify the most representative models for the region. Recognizing the inherent uncertainties in climate projections, as acknowledged by the IPCC (2000), necessitates ongoing efforts to refine modelling techniques and improve the reliability of local-scale predictions.

Analysis indicates a likely shift towards a wetter season in the watersheds (Table 8). Notably, several months are predicted to have significantly higher rainfall volumes, with potential increases reaching 42.87%. This necessitates

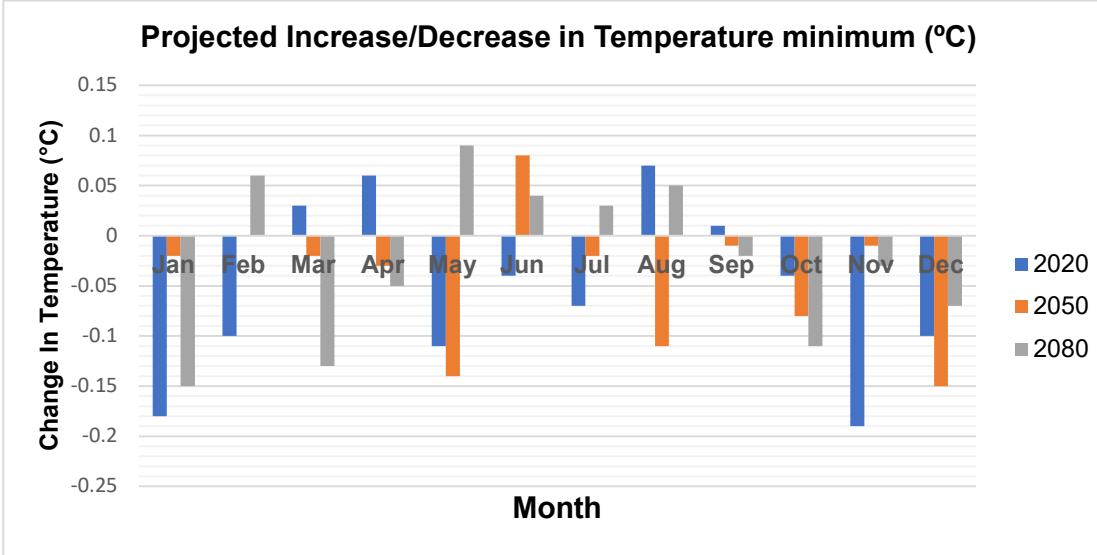

Fig. 6: Projected changes in mean monthly maximum temperature (°C).

Table 7: Mean monthly comparison and rate of change (increase/decrease) on the maximum temperature.

Month	Observed data	Temperature Maximum					
		Centigrade (^{0}C)			Increase/Decrease		
		2020	2050	2080	2020	2050	2080
Jan	30.57	30.67	30.47	30.64	0.10	**-0.10**	0.07
Feb	30.86	30.74	30.86	30.77	**-0.12**	0.00	**-0.09**
Mar	31.49	31.54	31.60	31.46	0.05	0.11	-0.03
Apr	32.06	32.13	32.14	32.15	0.07	0.08	0.09
May	31.65	31.71	31.65	31.75	0.06	0.00	0.11
Jun	30.94	30.97	31.04	31.01	0.03	0.10	0.07
Jul	30.57	30.52	30.69	30.66	**-0.06**	0.12	0.08
Aug	30.45	30.45	30.50	30.46	0.00	0.04	0.01
Sep	30.63	30.63	30.57	30.61	**-0.01**	**-0.07**	**-0.03**
Oct	30.94	30.93	31.00	30.88	**-0.02**	0.06	**-0.06**
Nov	31.11	31.19	31.12	31.10	0.08	0.01	**-0.01**
Dec	30.56	30.39	30.45	30.45	**-0.17**	**-0.11**	**-0.10**

proactive disaster risk management strategies, including the development of effective early warning systems for floods and landslides. The agricultural sector must respond by adapting cropping patterns and choosing appropriate crops. Conversely, industries like hydroelectric power plants can capitalize on the increased water availability.

Modelling Hydrologic Responses using the BROOK90 Hydrological Model

This section measured how changing climate influences the hydrological processes with the given land cover and other associated parameters. In projecting water quantity, this paper assumes that no changes shall be made to the land cover. The watersheds comprise 15 land covers and are further narrowed down to four major land cover classifications. As shown on Fig. 3, the area is dominated with Brushland (agroforestry, shrubs, and brushes) constituting 23313.9 hectares (59.10%), Bare lands (urban, harvested rice fields, open areas, and exposed soil) constituting 5623.9 hectares (14.26), forest constitutes 4,864.6 hectares (12.33%), and Grassland (rice fields and wastelands) constitutes another 4,025.5 (10.2%).

One focus of this study is the quantification of groundwater (seepage) since it is deemed essential in analyzing water supply, as water is being mined from the

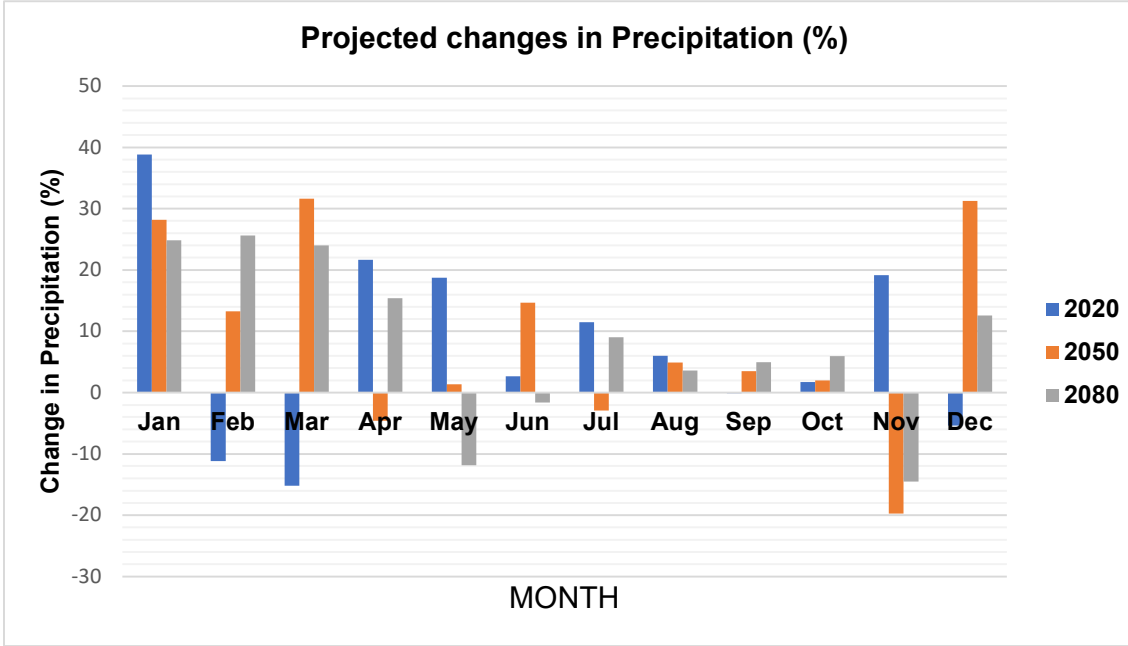

Fig. 7: Projected changes in precipitation (%).

Table 8: Mean monthly comparison and percent change in the amount of precipitation.

Month	Observed data	Precipitation					
		(mm)			Increase/Decrease (%)		
		2020	2050	2080	2020	2050	2080
Jan	128	178	164	160	38.79	28.15	24.84
Feb	81	72	91.8	102	**-11.18**	13.25	25.62
Mar	101	86	133	126	**-15.17**	31.62	23.97
Apr	170	207	162	196	21.68	**-4.59**	15.38
May	276	327	279	243	18.73	1.35	**-11.85**
Jun	292	300	335	288	2.63	14.65	**-1.63**
Jul	217	241	210	236	11.49	**-2.94**	9.04
Aug	248	262	260	256	5.97	4.88	3.57
Sep	219	219	227	230	**-0.10**	3.46	4.95
Oct	210	213	214	222	1.70	1.97	5.94
Nov	177	211	142	151	19.15	**-19.73**	**-14.52**
Dec	141	134	186	159	**-5.42**	31.26	12.55

groundwater. Essential to this modelling is the calibration and validation process. It is a prerequisite for the fitness of the model that all predictors need to be fit, and fitness will only be acceptable when these are further subjected to statistical analysis, where values are acceptable (RMSE and Nash Sutcliffe).

This study utilized streamflow data from two distinct watersheds, the Talomo and Lipadas watersheds. Each dataset was split into two parts for model calibration and validation. Climate data for both watersheds were derived from a single source: the Bago Oshiro Agrometeorological Station, situated within the Talomo Watershed. The average annual precipitation was 2873.83 mm during the calibration period and 2858.8 mm during the validation period.

Average annual streamflow varied between calibration and validation periods for both watersheds. In the Talomo

Table 9: BROOK90 model simulation in Mt. Talomo-Lipadas Watersheds.

Watersheds	Performance criteria	Calibration	Validation
Talomo	R^2	0.979	1.000
	Nash-Sutcliffe	0.845	0.621
Lipadas	R^2	1.000	1.000
	Nash-Sutcliffe	0.622	0.836

watershed, streamflow was 1251.70 mm during calibration and increased to 1412.45 mm during validation. The Lipadas watershed saw a decrease, from 1088.83 mm during calibration to 907.03 mm during validation.

A high coefficient of determination (R^2) value, as shown in Table 9 and Figs. 8 and 9, indicates a strong annual relationship between measured and simulated streamflow. This metric (ranging from 0 to 1) reflects the model's predictive skill, quantifying the proportion of streamflow variability captured. Positive Nash-Sutcliffe coefficients further validate the model's performance. However, the model's sensitivity was insufficient to accurately simulate monthly and daily streamflow. Despite this limitation, considering the limited availability of climate and streamflow data in the region, this simulation represents the best achievable outcome. Results for calibration and validation were obtained by averaging across four land cover types, employing appropriate parameters, especially for canopy characteristics, as suggested by the BROOK90 model (Federer, 2002).

Considering the limited availability of observed streamflow and climate data, the model validation achieved a higher coefficient of determination, indicating a better fit to observed data than the calibration period for both watersheds.

Projected Recharge (Seepage) of Talomo-Lipadas Watersheds

In the BROOK90 model, recharge, the water withdrawn primarily by the Davao Water District to supply 99% of the urban population, is calculated as precipitation minus evaporation and flow. Precipitation is the primary source of all water in the terrestrial phase of the hydrologic cycle (Satterlund 1972, cited in Combalicer et al. 2010).

Analysis of recharge data from 1997 to 2006 across the two watersheds revealed an annual average of 134.06 million cubic meters (MCM). The lowest flow months were typically observed in March, while July experienced the highest flows.

Over the coming decades, as shown in Table 10 and Fig. 10, recharge is projected to decline. By 2020, a reduction of

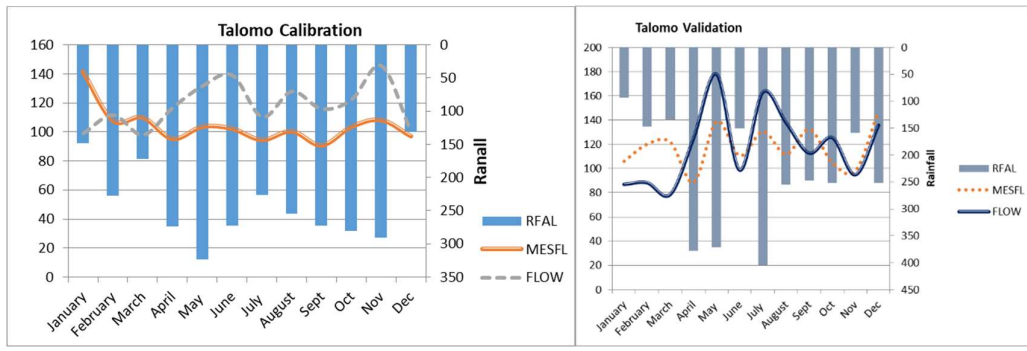

Fig. 8: Calibration Period for Talomo Watershed (left) and Validation Period for Talomo Watershed (right).

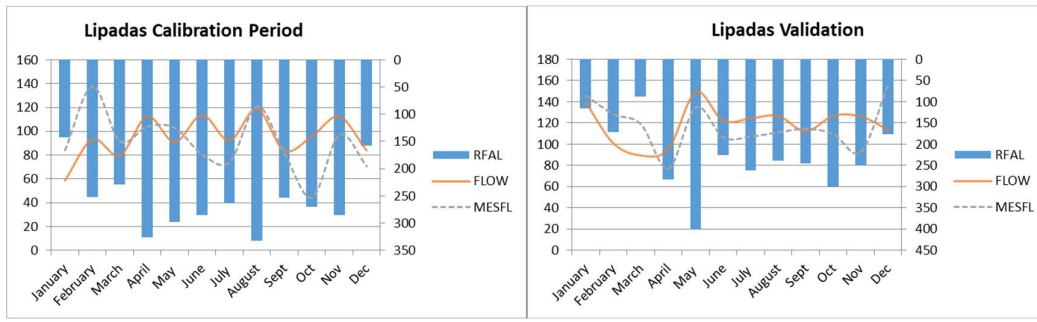

Fig. 9: Calibration Period for Lipadas Watershed (left) and Validation Period for Lipadas Watershed (RFAN- rainfall, MSFL- measured flow, FLOW- simulated flow).

-18.63% (25.1 MCM) is expected, with low flow from April to December, reaching a minimum of -55.29% (3.98 MCM) in April. In 2050, the reduction is projected to be -23.08% (31.07 MCM) continuously from March to December. By 2080, the decline reaches -25.84% (34.79 MCM), with low flow spanning the same period.

The results indicate a strong sensitivity of groundwater recharge in the Talomo-Lipadas Watersheds to climate change. A relatively small rise in maximum temperature, ranging from 0.10°C to 0.17°C, is sufficient to negatively impact water availability for recharge.

The projected decline in groundwater recharge, despite increased rainfall, is a serious concern for future water supplies. Reductions are projected to reach 18.63% by 2020, 23.08% by 2050, and 25.84% by 2080, highlighting the urgency of addressing this issue.

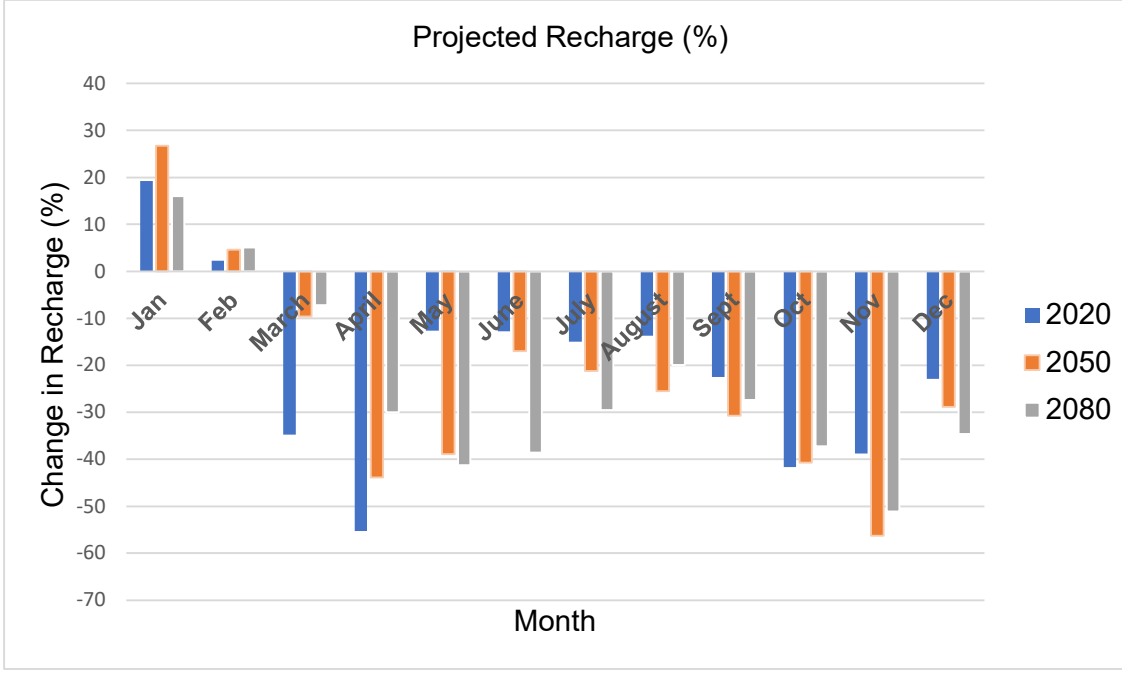

Fig. 10: Recharge changes in 2020, 2050, and 2080 in Percentage.

Table 10: Recharge to groundwater expressed in Million Cubic Meter (MCM) in three time slice periods for the two subwatersheds.

Months	Recharge [MCM]				% Increase/Decrease		
	OBS	2020	2050	2080	2020	2050	2080
Jan	11.82	14.1	14.98	13.71	19.25	26.71	16
Feb	8.97	9.18	9.39	9.43	2.27	4.60	5.06
March	6.30	4.12	5.70	5.86	-34.72	-9.66	-7.2
April	7.37	3.29	4.14	5.16	-55.29	-43.86	-30.01
May	11.77	10.28	7.18	6.91	-12.65	-38.97	-41.29
June	16.56	14.44	13.74	10.18	-12.8	-17.02	-38.53
July	15.55	13.22	12.25	10.96	-15.01	-21.24	-29.54
August	12.71	10.97	9.47	10.19	-13.72	-25.54	-19.88
Sept	12.24	9.49	8.48	8.89	-22.47	-30.72	-27.41
Oct	11.37	6.64	6.75	7.14	-41.64	-40.68	-37.22
Nov	9.85	6.04	4.31	4.82	-38.75	-56.29	-51.11
Dec	10.03	7.74	7.13	6.56	-22.89	-28.88	-34.58
Total	134.6	109.50	103.53	99.81	-18.63	-23.08	-25.84

The above findings are concurrent with a study conducted by Zektser & Loaiciga (1993), Bear & Cheng (1999), where climate has the potential to affect the quantity and quality of groundwater. Climate change and variability will have numerous effects on recharge rates and mechanisms (Vacarro 1992, Green et al. 2007). The impact of climate change on groundwater recharge is a subject of ongoing research, with many studies predicting declines (Herrera-Pantoja & Hiscock 2008). Kruger et al. (2001) provide an example, projecting a potential 30% reduction in a lowland aquifer in Germany.

The decline in groundwater recharge despite increased rainfall is attributed to a significant increase in evapotranspiration (ET) (Fasullo et al. 2015). Rising temperatures, associated with climate change, have led to higher potential ET. Additionally, Morris et al. (2017) changes in land cover, such as deforestation, have reduced canopy interception and increased soil evaporation (Famiglietti 2014). Soil moisture indicates that a larger proportion of rainfall is being lost through ET, leaving less water available for infiltration and recharge. This is supported by process-based modelling, which shows a strong correlation between increased temperatures and reduced recharge, even with increased precipitation.

The dynamic nature of groundwater recharge, driven by precipitation variability, can have cascading effects on groundwater systems. These include impacts on aquifer yield and discharge, along with potential shifts in flow regimes, such as the conversion of gaining streams to losing streams and adjustments to groundwater divides. Also, Green et al. (2011) simulated that recharge is highly dependent on the combination of soil and vegetation type.

Land use and land cover changes (LULC) significantly influence groundwater storage by altering key hydrological processes such as infiltration, evapotranspiration, and runoff. In the Talomo-Lipadas Watersheds, the dominant land cover type is Brushland (59.10%), followed by Bare lands**,** Forest**,** and Grassland. Increasing bare land cover contributes to higher surface runoff, which not only reduces infiltration but also leads to soil erosion, further reducing the watershed's ability to retain water. These land cover classifications play a crucial role in groundwater recharge (seepage) and, consequently, in the sustainability of water resources.

Also, in urbanized and bare land areas, impervious surfaces like roads, buildings, and compacted soil prevent water from infiltrating; as a result, more precipitation is lost as surface runoff rather than recharging groundwater reserves. Observed deforestation in the area disrupts the natural infiltration cycle, reducing the soil's ability to retain water and gradually release it into aquifers. According to Paul (2006), groundwater recharge is significantly influenced by land cover. Paul (2006) also noted considerable variation in recharge rates depending on land use, with low recharge in settlements—caused by impervious surfaces and infrastructure—contrasting sharply with the high recharge observed in forested areas. This highlights the critical role of forests in maintaining groundwater supplies and the vulnerability of these resources to human development.

Groundwater recharge (seepage) is strongly influenced by land cover. In this watershed, brushland is the predominant land cover, constituting 59.10% of the total area. Research by Paul (2006) has demonstrated the significant variation in groundwater recharge across different land uses. Specifically, settlement zones, due to extensive impervious surfaces and infrastructure, experience minimal recharge, whereas natural or near-natural forested areas receive the highest levels. This highlights the critical role of forest vegetation in maintaining groundwater resources and the detrimental effects of anthropogenic activities on these systems.

CONCLUSIONS

This research directly addresses the need for local-level studies on climate change impacts, a call echoed internationally and nationally. Literature on this topic is limited, particularly in developing nations and specifically within the Philippines. In Davao City, the reality of climate change's effects on water resources, particularly groundwater availability, is evident. Using the Statistical Downscaling Method, climate scenarios for both minimum (Tmin) and maximum temperatures (Tmax) increase over time. Of greater concern is the projected rapid increase in precipitation. These results highlight the potential for both water shortages and increased risks of floods and landslides, requiring immediate attention from all sectors related to climate and water.

Using the BROOK90 hydrological software, it projects a decline in seepage due to the combined effects of climate change, land cover alterations, and other relevant parameters. The resulting monthly, annual, and time-slice recharge data provide valuable information for various stakeholders. This information will be crucial in designing, planning, and implementing water conservation strategies, especially for the Davao City Water District (DCWD) as they plan for future water sourcing to meet the needs of the city's expanding population.

Based on the compelling empirical evidence presented, the full integration of the downscaled, station-scale climate scenario is strongly recommended across all climate and water-related sectors within the Talomo-Lipadas Watershed. This information should be foundational to all planning and development initiatives, ensuring climate resilience and water

security. Disaster risk reduction and management agencies should leverage these findings for proactive preparedness against potential extreme weather events. To enhance the robustness of future projections, expanding the weather station network and employing multi-model approaches for both climate downscaling and hydrologic modelling are essential for validation. Furthermore, maximizing recharge data collection is critical for developing a comprehensive, 100-year water adaptation strategy that secures sustainable domestic water supplies, while also addressing the needs of agriculture, industry, and ecosystem health, in the face of increasing population and economic activity.

An integrated water resource management (IWRM) framework, incorporating stakeholder engagement and participatory decision-making, is essential for sustainable water management in Davao City. This framework should be based on scientific data and incorporate local knowledge and values. Multi-stakeholder platforms, involving government agencies, water utilities, NGOs, and community groups, should be established to facilitate the development and implementation of water management plans. Results from hydrological modeling and water quality assessments should be communicated effectively to the public to raise awareness about water-related risks and promote water conservation.

When facing a projected recharge decline, particularly in a context like Davao City, a combination of adaptive strategies is essential. Managed Aquifer Recharge (MAR) and afforestation are two key approaches. Another suggestion is the source water diversification, targeted reforestation in recharge areas, and riparian zone restoration, among others. By implementing these adaptive strategies, Davao City can enhance its resilience to projected recharge decline and ensure long-term water security.

ACKNOWLEDGMENTS

The successful completion of this research was greatly facilitated by the insightful guidance of the advisory committee, composed of Dr. Juan M. Pulhin, Dr. Rex Cruz, Dr. Rodel D. Lasco, and Dr. Carmelita M. Rebanocos. I am also deeply grateful for the expert tutoring provided by Dr. Edwin Combalicer and Francis John Federoga in the application of the BROOK90 hydrological model and SDSM.

I extend my sincere thanks to the Davao City Water District and the PAG-ASA Meteorological Station at Bago Oshiro, Davao City, for generously providing essential data.

I am further thankful to the Commission on Higher Education (CHED) for the scholarship and dissertation financial support. I am also indebted to the International Development and Research Center (IDRC), along with its partner institution, the University of Nairobi, for the invaluable opportunity and financial assistance that enabled the completion of this study.

REFERENCES

Bamala, A., Uddin, M.G. and Olbert, A.I., 2024. Harnessing machine learning for assessing climate change influences on groundwater resources: A comprehensive review. *Heliyon*, 10(17), e37073. DOI

Bates, B., Kundzewicz, Z.W., Wu, S. and Palutikof, J.P., 2008. *Climate Change and Water*. Technical Paper VI of the Intergovernmental Panel on Climate Change. Intergovernmental Panel on Climate Change Secretariat, Geneva, pp.210.

Branzuela, N.E., Faderogao, F.J.F. and Pulhin, J.M., 2015. Downscaled projected climate scenario of Talomo-Lipadas watershed, Davao City, Philippines. *Journal of Earth Science & Climate Change*, 6(268), pp.1–10. DOI

Benz, S.A., Irvine, D.J., Rau, G.C., Bayer, P., Menberg, K., Blum, P., Jamieson, R.C., Griebler, C. and Kurylyk, B.L., 2024. Global groundwater warming due to climate change. *Nature Geoscience*, 17(6), pp.545–551. DOI

Combalicer, E.A., Cruz, R.V.O., Lee, S. and Im, S., 2010. Assessing climate change impacts on water balance in the Mount Makiling Forest, Philippines. *Journal of Earth Science*, 119(3), pp.265–283.

Hearne, D., 2011. *Customized IWRM Guidelines for Davao City and Region*. First Edition. HELP Davao Network.

Dao, P.U., Heuzard, A.G., Le, T.X.H., Zhao, J., Yin, R., Shang, C. and Fan, C., 2024. The impacts of climate change on groundwater quality: A review. *Science of the Total Environment*, 912, p.169241. DOI

Davamani, V., John, J.E., Poornachandra, C., Gopalakrishnan, B., Arulmani, S., Parameswari, E., Santhosh, A., Srinivasulu, A., Lal, A. and Naidu, R., 2024. A critical review of climate change impacts on groundwater resources: A focus on the current status, future possibilities, and role of simulation models. *Atmosphere*, 15(1), p.122. DOI

Dettinger, M.D. and Earman, S., 2007. Western groundwater and climate change—pivotal to supply sustainability or vulnerable in its own right? *Ground Water*, 45(1), pp.4–5. DOI

Famiglietti, J.S., 2014. The global groundwater crisis. *Nature Climate Change*, 4(11), pp.945–948. DOI

Fasullo, J.T., Trenberth, K.E., Walsh, J.E. and Washington, W.M., 2015. Global warming of the climate system. *Reviews of Geophysics*, 53(3), pp.450–483. DOI

Federer, C.A., Vörösmarty, C. and Fekete, B., 2003. Sensitivity of annual evaporation to soil and root properties in two models of contrasting complexity. *Journal of Hydrometeorology*, 4(6), pp.1276–1290. DOI

Ficklin, D.L., Letsinger, S.L., Stewart, I.T. and Maurer, E.P., 2018. Projected climate change impacts on streamflow in the western United States. *Journal of Hydrology*, 564, pp.976–993. DOI

Flatto, G.M. and Boer, G.J., 2001. Warming asymmetry in climate change simulations. *Geophysical Research Letters*, 28(10), pp.195–198. DOI

Green, T.R., Taniguchi, M., Kooi, H., Gurdak, J.J., Allen, D.M., Hiscock, K.M., Treidel, H. and Aureli, A., 2007. Beneath the surface of global change: Impacts of climate change on groundwater. *Journal of Hydrology*, 405(3-4), pp.532-560.

Green, T.R., Taniguchi, M., Kooi, H., Gurdak, J.J., Allen, D.M. and Hiscock, K.M., 2011. Beneath the surface of global change: Impacts of climate change on groundwater. *Journal of Hydrology*, 405(3-4), pp.532-560. DOI

Hatfield, J.L. and Prueger, J.H., 2015. Temperature extremes: Effect on plant growth and development. *Weather and Climate Extremes*, 10, pp.4-10. DOI

Intergovernmental Panel on Climate Change (IPCC), 2000. *IPCC Special Report Emissions Scenarios*. *Summary for Policy Makers*. IPCC. Link

Intergovernmental Panel on Climate Change (IPCC), 2021. *Climate Change 2021: The Physical Science Basis*. Contribution of Working Group I to the Sixth Assessment Report of the Intergovernmental Panel on Climate Change. Cambridge University Press. DOI

Kozak, A. and Kozak, R., 2003. Does cross validation provide additional information in the evaluation of regression models? *Canadian Journal of Forest Research*, 33(6), pp.976-987.

Kruger, A., Ulbrich, U. and Speth, P., 2001. Groundwater recharge in North Rhine-Westphalia predicted by a statistical model for greenhouse gas scenarios. *Physics and Chemistry of the Earth, Part B: Hydrology, Oceans and Atmosphere*, 26(11-12), pp.853-861. DOI

Kundzewicz, Z.W., Mata, L.J., Arnell, N.W., Doll, P., Kabat, P., Jimenez, B., Miller, K.A., Oki, T., Sen, Z. and Shiklomanov, I.A., 2007. Freshwater resources and their management. In: Parry, M.L., Canziani, O.F., Palutikof, J.P., van der Linden, P.J. and Hanson, C.E. (eds.) *Climate Change 2007: Impacts, Adaptation and Vulnerability*. Cambridge University Press, Cambridge, pp.173-210.

Kiniry, J.R., 2012. *Input documentation for SWAT2012*. USDA Agricultural Research Service and Texas A&M AgriLife Research.

Morris, C.E., Simmonds, I. and Plummer, N., 2017. Quantifying the impact of observed land cover change on the Australian climate. *Geophysical Research Letters*, 44(14), pp.7461-7468. DOI

Nyeko-Ogiramoi, P., Ngirane-Katashaya, G., Willems, P. and Ntegeka, V., 2010. Evaluation and inter-comparison of global climate models' performance over Katonga and Ruizi catchments in Lake Victoria basin. *Physics and Chemistry of the Earth, Parts A/B/C*, 35(15-18), pp.618-633.

Paul, M.J., 2006. Impact of land-use patterns on distributed groundwater recharge and discharge. *Chinese Geographical Science*, 16(3), pp.229-235. DOI

Parmesan, C. and Yohe, G., 2003. A globally coherent fingerprint of climate change impacts across natural systems. *Nature*, 421(6918), pp.37-42. DOI

Philippines Environment Monitor, 2003. *Philippines Environment Monitor 2003*. Retrieved 9 Apr. 2025 from www.worldbank.org.ph

Rosenzweig, C., Iglesius, A., Yang, X.B., Epstein, P.R. and Chivian, E., 2001. Climate change and extreme weather events - Implications for food production, plant diseases, and pests. *NASA Publications*, 24. Link

Satterlund, D.R., 1972. *Wildland Watershed Management*. New York: The Ronald Press Co.

Tubiello, F.N., 2007. Effects of climate change on agricultural production. *European Journal of Agronomy*, 26(4), pp.449-462. DOI

Vacarro, J.J., 1992. Sensitivity of groundwater recharge estimates to climate variability and change, Columbia Plateau, Washington. *Journal of Geophysical Research*, 97(D3), pp.2821–2833.

Vorobevskii, I.I., 2020. R-based framework for BROOK90 hydrological model: Implementation and application for forested catchment. *Environmental Modelling & Software*, 132, p.104800. DOI

Wilby, R.L., Dawson, C.W. and Barrow, E.M., 2002. SDSM—a decision support tool for the assessment of regional climate change impacts. *Environmental Modelling & Software*, 17(2), pp.147–159.

Wu, W., Lo, M., Wada, Y., Famiglietti, J.S., Reager, J.T., Yeh, P.J., Ducharne, A. and Yang, Z., 2020. Divergent effects of climate change on future groundwater availability in key mid-latitude aquifers. *Nature Communications*, 11(1), pp.1–9. DOI

Zektser, I.S. and Loaiciga, H.A., 1993. Groundwater fluxes in the global hydrologic cycle, past, present, and future. *Journal of Hydrology*, 144(1–4), pp.405–427.